AIAA 80-1318R

Modeling of the Interaction of 10.6 μm Laser Radiation with Reinforced Plastics

A. Ballantyne,* J. A. Woodroffe,* and T. L. Cronburg*
Avco-Everett Research Laboratory, Inc., Everett, Mass.
R. R. Rudder†
Air Force Weapons Laboratory, Albuquerque, N. Mex.
and
M. J. Bina‡
Lockheed Missiles and Space Company, Sunnyvale, Calif.

The objective of this work was to develop a phenomenological model of pulsed CO_2 laser interaction with reinforced composite materials. Experimental observation has shown that the multilayer composite material delaminates under pulsed CO_2 laser irradiation. This is a consequence of the energy storage mechanism arising out of a finite absorption depth to the laser radiation. A heat transfer model was developed to describe the observed delamination behavior of the composite materials. Good agreement was obtained between the model predictions and experimental data. The model has been used to extrapolate to high average power irradiation.

Nomenclature

c = specific heat
E_R = residual fluence
E_{R_0} = residual fluence for surface at ambient temperature
E_V = heat of varporization
h = laminate thickness
R = pulse repetition frequency
t = time
T = absolute temperature
T_0 = ambient temperature
x = distance from target surface
α = thermal diffusivity
Δ = laminate displacement
Δu = velocity differential across laminate
Δp = differential pressure
δ = constant in Eq. (5)
ρ = material density
λ = conduction depth
λ_a = absorption depth for laser radiation
θ = temperature, $=T-T_0$
τ = shear stress in laminate
μ = glass viscosity
η = heat transfer parameter, $=x/(2\sqrt{\alpha t})$
ξ = heat transfer parameter, $=E_{R_0}R/[\rho c\alpha\theta_v]$
ζ = mass removal parameter in Eq. (19)
ω = $\sqrt{\alpha t}/\lambda$

Subscripts

D = delamination
V = vaporization
R = removal

Presented as Paper 80-1318 at the AIAA 13th Fluid and Plasma Dynamics Conference, Snowmass, Colo., July 14-16, 1980; submitted Aug. 1, 1980; revision received Dec. 8, 1980.

*Principal Research Scientist. Member AIAA.
†Research Physicist. Member AIAA.
‡Staff Scientist. Member AIAA.

Introduction

IN recent years, the advent of high powered lasers has enabled existing regimes of material heating to be extended to much higher heating rates. From the viewpoint of material processing, the laser has been used primarily for heating of metals. This study was undertaken to examine the mechanisms of reinforced plastic heating under high average power. This is of particular interest as the physics of the laser absorption are significantly different from metallic materials; for glasses and polymers, the absorption depth of laser radiation is comparable to the laser wavelength at 10.6 μm.

The objective of this work was to develop a model capable of describing the interaction processes occurring in the irradiation of glass fiber reinforced composite materials by a pulsed CO_2 laser. In particular we examined the mechanism of the experimentally observed ply delamination. In order to model such behavior, a semi-analytical treatment was pursued, using relevant experimental data for empirical inputs as required. The model is used to extrapolate from the existing data base to higher laser repetition frequency regimes.

Figure 1 illustrates the complete range of phenomena possible in an interaction between a pulsed laser and a reinforced composite material. The incident energy may couple either directly to the surface, or, if the flux is sufficiently high, by plasma reradiation. The plasma formation will typically reduce the coupled fluence as compared to low flux coupling. However, the high pressure plasma will result in an impulsive loading to the surface that may cause mechanical damage. The absorbed energy can contribute to two mechanisms of mass removal: 1) "prompt" mass removal from the surface in the form of resin pyrolysis or glass vaporization and 2) "residual fluence" induced mass removal resulting from in depth absorption of the coupled fluence and conduction into the composite matrix.

The residual fluence results in an interpulse pyrolysis from within the target material, that results in weakening of the structural integrity of the uppermost laminate, allowing delamination to occur. In addition, at low air flow shear velocity, a combustion wave may be stabilized in the boundary layer.

At high surface temperatures and high average fluxes it may be possible for a flowing melt layer to occur, causing ad-

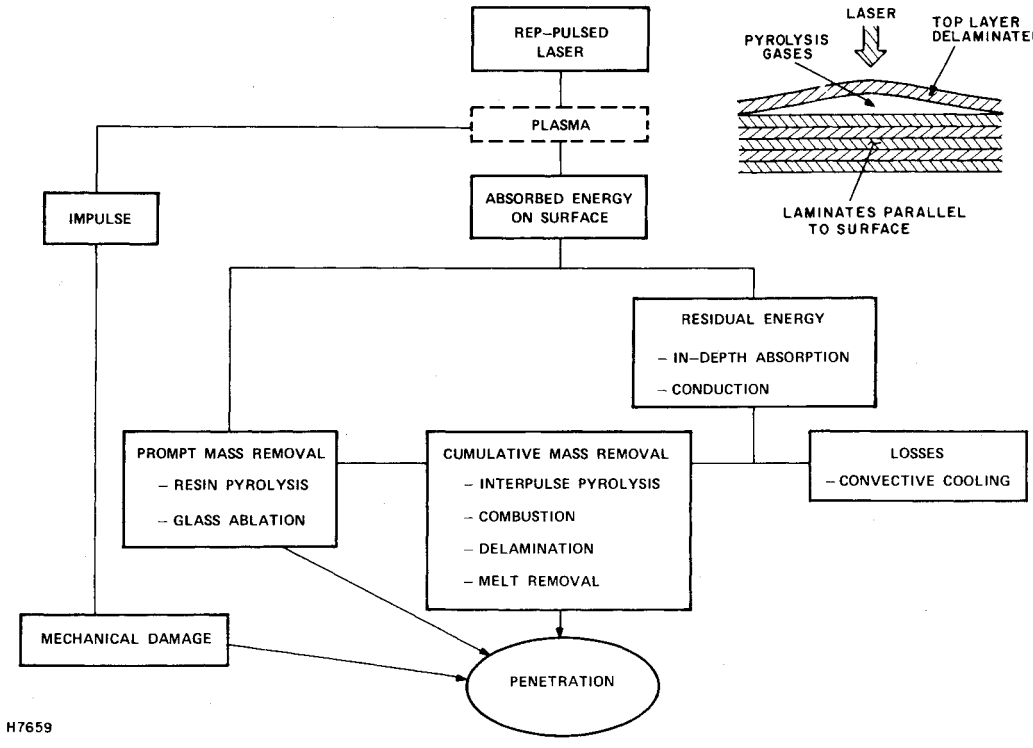

Fig. 1 Phenomenology of pulsed laser interaction with composite materials.

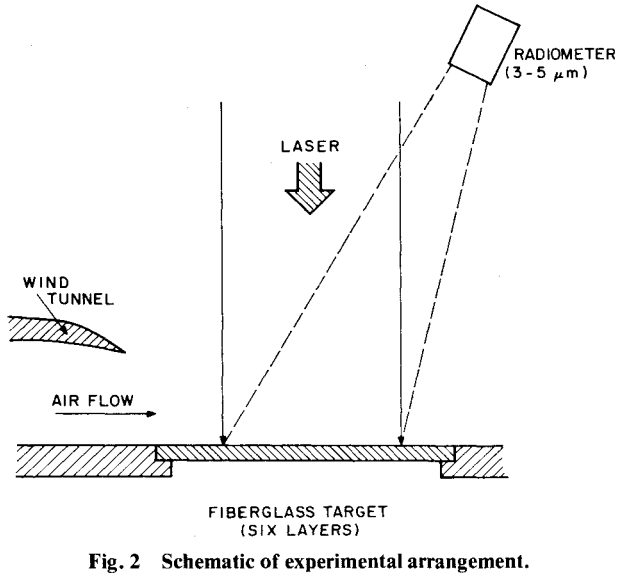

Fig. 2 Schematic of experimental arrangement.

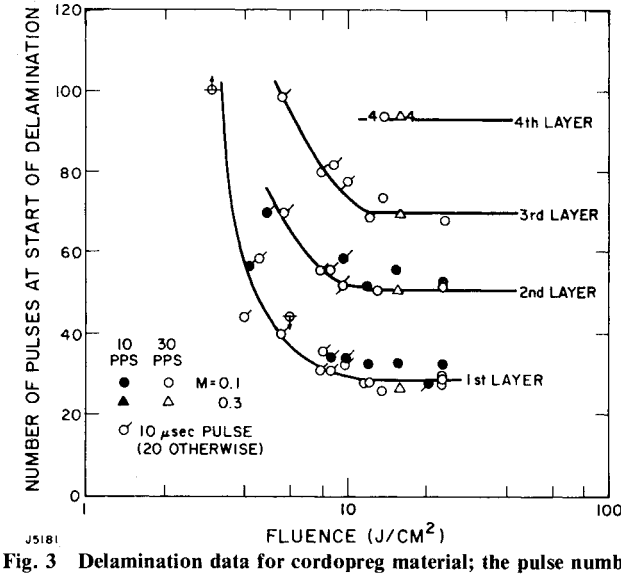

Fig. 3 Delamination data for cordopreg material; the pulse number is for the observable start of delamination for each layer.

ditional mass loss. However, all indications are that delamination and vaporization are the dominant mechanisms. Therefore, in this work we consider only delamination and vaporization. Convective cooling losses are assumed negligible for modeling purposes which is a reasonable approximation for the conditions of interest.

Experimental Observations

The experiments were performed with an electron beam sustained repetitively pulsed CO_2 laser capable of 30 Hz operation. The pulse length was between 10 and 20 μs, and fluxes in the range 10^5-10^6 W/cm^2. The target geometry is shown in Fig. 2. The composite material consists of a number of woven mats of glass laid parallel to the surface which are bonded with a polymer resin filler. Irradiation was normal to the surface, and a debris cleaning air curtain flowed across the target. The laser flux distribution across the spot was fairly uniform. This was achieved by overlapping eight segments of the laser beam at the target plane.

The target diagnostics consisted of high speed cine cameras and an i.r. pyrometer for front surface temperature measurement. Typical test shots consisted of 70-100 pulse bursts of laser radiation. Pulse fluences were typically in the range 1-20 J/cm^2.

The primary observation was that of target delamination, with each ply of the target becoming detached sequentially from the underlying layers, undergoing a breakup and removal, which exposed the subsequent layer to the radiation. This process was observed to correlate with pulse fluence. (See Fig. 3 discussed below.) At low fluences, the number of pulses to the onset of delamination (observed to be a bubbling or cracking of the target surface) was observed to fall with increasing fluence. At higher fluences, the number of pulses is observed to be essentially constant.

This process is a consequence of absorption of laser energy by the surface, and conduction of thermal energy into the material, with subsequent pyrolysis and degradation of the polymer binder. This allows the topmost layer to become

detached from the remaining layers. It is then torn off by airflow across the surface and/or disintegrates under further irradiation.

The detailed surface energy absorption process is complex and not well characterized at this juncture. Essentially, the in depth absorption of the radiation by the glass (absorption depth of order 10 μm) results in significant energy deposition and storage in the target material, with surface vaporization rate and surface temperature limiting further accumulation. This "residual fluence" concept[1,2] is pivotal to the model development.

Figure 3 illustrates the typical behavior of target under the action of laser irradiation at 10 and 30 Hz repetition frequency. With increasing fluence per pulse, the number of pulses to the onset of delamination is reduced until the fluence reaches a value of approximately 7-9 J/cm^2. At this point increasing fluence does not change the essentially constant number of pulses to the onset of delamination. (If a plasma is formed above the target, the coupled fluence to the surface is reduced and the number of pulses to delamination onset is increased corresponding to those below plasma threshold. For reasons of clarity, these data points are not shown in Fig. 3.)

The layer, on becoming detached from the underlying structure, does not break away instantaneously. There is a finite time over which the layer breaks up into smaller pieces that are cleared by the curtain flow. The number of pulses required to clear the layer from half of the irradiated spot is shown in Fig. 4. As can be seen there is significant scatter in the data. This is almost certainly a function of the detailed mechanical stress patterns and their statistical variance, induced in the target by the irradiation. The mechanics of this process are not clearly understood at this time. From these data it is possible to make a reasonable estimate of removal time for modeling purposes; a value of 5 pulses was used to approximate the mean removal time.

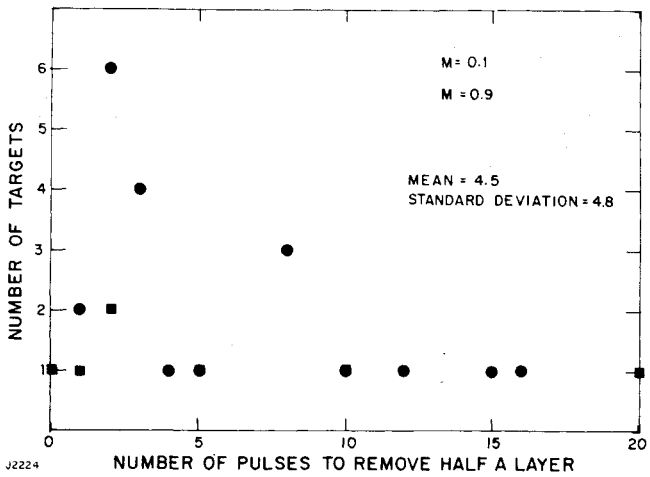

Fig. 4 Layer removal times for the onset of delamination.

A typical example of the temperature history during irradiation at 30 Hz is shown in Fig. 5. The temperature reaches approximately 1500 K before the first layer starts to detach and disintegrate. The dip in temperature correlates well with visual observation of the onset delamination. For a complete instantaneous layer removal, at a finite number of pulses after detachment from the substrate, a much larger dip in temperature would be expected. However, the finite removal time, coupled with the spot integrated surface temperature measurement results in a much smaller observed temperature change.

Model Formulation

The model is based upon an analytic description of heat transfer in the glass fiber structure. The energy source for the model is given by the product of residual fluence and repetition frequency,

$$\phi_{avg} = E_R R \tag{1}$$

This is the effective average flux, which is, in general, less than the incident flux. As we are interested predominantly in the thermal history deep inside the target, ignoring the precise pulsed thermal history is admissible, allowing simplification of the problem. From experimental data at low repetition frequency, E_R has been evaluated to be approximately 7-9 J/cm^2. However, it is physically reasonable that increasing surface temperature may significantly affect energy deposition by a subsequent pulse, reducing the amount of energy deposited before vaporization occurs. Therefore, two models of residual energy were used; a constant value and one that falls linearly with increasing surface temperature. The second model can be explained via the finite absorption depth λ_a giving a residual energy of

$$E_R = \rho c \lambda_a (\theta_v - \theta_s) \tag{2}$$

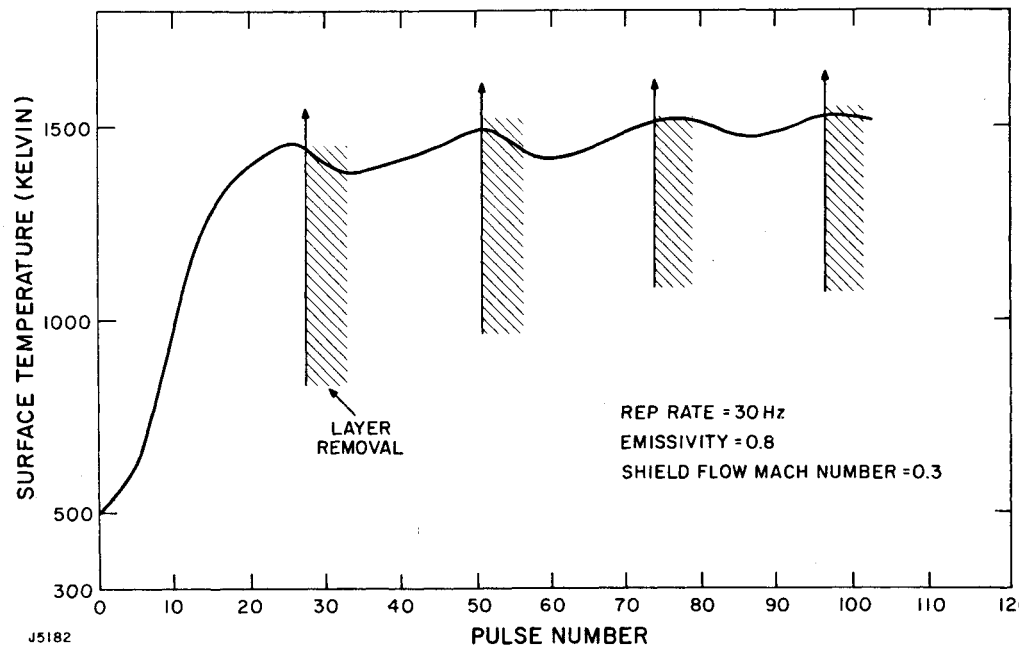

Fig. 5 Representative example of surface radiometry data.

where θ_s is the surface temperature prior to irradiation by the pulse. (This is neglecting conduction during the laser pulse.) The initial residual energy, for ambient surface temperature is thus

$$E_{R_0} = \rho c \lambda_a \theta_v \tag{3}$$

giving

$$E_R = E_{R_0}(\theta_v - \theta_s)/\theta_v \tag{4}$$

The exact behavior of the energy absorption by the glass fibers has not yet been well characterized. This is a consequence of undefined properties of glasses at very high temperatures. There is evidence of large increases in thermal conductivity at high temperatures.[3] The absorption depth of the material is also likely to vary strongly with temperature. This is evidenced by the work of Edwards[4] who measured absorption coefficients of quartz glasses in the 300-1250 K temperature range, for wavelength 0.17-3.5 μm. With the exception of molecular absorption bands the glasses exhibited an approximately linear increase of absorption coefficient with increasing temperature. Thus

$$\lambda(\theta) \sim 1/\theta$$

Without precise data for 10.6 μm irradiation at elevated temperatures it becomes difficult to assess the temperature variation of $E_R(\theta)$. The assumed linear variation would appear, however, to be a reasonable physical model of the process.

In order to account for finite conduction of heat into the material, due to temperature gradient, when the surface reaches a quasisteady vaporization condition, the residual energy model is taken, heuristically, to be

$$E_R = E_{R_0}\left(\delta + \frac{\theta_v - \theta(0,t)}{\theta_v}\right) \tag{5}$$

where δ is a small constant; δ is a consequence of finite conduction into the material even if the surface is at vaporization temperature.

The data would indicate that the residual fluence is between 7-9 J/cm^2. For purposes of this model, the value of E_{R_0} is taken as 8.5 J/cm^2. This corresponds to an average value of approximately 7 J/cm^2 for the 10 and 30 Hz irradiations ($T_D \sim 1500$ K). Use of the analytical model described in the following sections results in the surface reaching vaporization prior to delamination for an average flux of order 10^4 W/cm^2. This gives an estimated value of $\delta \simeq 0.1$.

The heat transfer analysis considers a semi-infinite target comprised of layers of thickness h. The model is one dimensional. The initial temperature history is thus

$$\theta(x,t) = f(x,t,\alpha,E_R,\rho c)$$

where α is the thermal diffusivity, and ρc the volumetric specific heat. Obviously we are dealing with an in depth chemically reacting medium, and no explicit description of pyrolysis behavior is put in the model. However, energetically it is implicit in the evaluation of ρc, whereby the endothermic pyrolysis energy has been included to give an effective specific heat. Thus, we can write approximately

$$(\rho c)_{\text{effective}} \simeq f_p[(\rho c)_p \theta_D + H_p]/\theta_D + (1 - f_p)(\rho c)_g \tag{6}$$

where H_p is the heat of pyrolysis, f_p the polymer glass fraction and θ_D the temperature rise at the rear of the laminate. On loss of pyrolysis gases, the effective volumetric specific heat of the remaining glass does not change substantially. This is a consequence of the increase in glass specific heat with temperature. Thus, a constant value volumetric specific heat appears a reasonable first-order approximation. This was evaluated to be approximately 2.5 J/cm^3, for $\theta_D \sim 800$ K, $H_p \sim 1000$ J/gm, and $f_p \sim 0.3$.

The pyrolysis of polymer is necessary for delamination. The strong exponential decomposition rate dependence on temperature makes it possible to approximate the behavior with a simple criterion. Delamination occurs subsequent to layer detachment when the rear surface of the ply reaches a "delamination temperature," at which point all of or most of the polymer has been pyrolyzed. The exact criterion for separation of the layer from the rest of the target has not been firmly established. One possible criterion is that of pyrolysate gas pressure buildup under the layer, causing stress failure of the fibers. Also, the effect of airflow across the surface will be to cause a pressure differential across the layer. This pressure differential induces a shear flow of the fiber layers. A simplified model of the flow of the glass can be constructed, by considering the pressure to induce a cylindrical distortion of the laminate.

The shear stress τ induced in the flowing glass is related to the pressure difference across the laminate by the relationship

$$\Delta p \simeq \frac{\tau h \Delta}{D(1 + 4\Delta^2/D^2)} \tag{7}$$

where Δ is the maximum displacement of the laminate, and the strain in the layer is given by

$$\epsilon = 4\Delta^2/D^2 \tag{8}$$

The shear stress is related to the velocity differential across the laminate given by

$$\Delta u \simeq \frac{4h}{D}\frac{d\Delta}{dt} \tag{9}$$

Thus the shear stress is given by

$$\tau \simeq \mu \frac{\Delta u}{h} \simeq \frac{4\mu}{D}\frac{d\Delta}{dt} \tag{10}$$

Solving Eqs. (7) and (9) gives a failure time

$$t_{\text{fail}} \simeq \frac{4\mu h}{\Delta p D} \ell n(1 + \epsilon_{\text{fail}})$$

Typically the experiments at 10 Hz and 30 Hz took 5 pulses to partially clear a layer ($\geq 50\%$ of the spot area). The layer thickness was 275 μm and spot dimension 5 cm. For an assumed strain of order 0.5 and a mean layer temperature of 1200 K, corresponding to a viscosity of order 10^6 P, the required pressure differential is of order 5×10^3 N/m^2. The aerodynamic pressure difference corresponding to a Mach number of 0.1 is 1500 N/m^2. The contribution of pyrolysis gases would generate a larger total pressure difference. This implies that pressure generated removal is a plausible mechanism.

Solution of the Heat Transfer Equation

The model considered here consists of conduction of the residual fluence into the target with no radiation or convective losses. The conduction equation is given in the form

$$\frac{\partial \theta}{\partial t} = \alpha \frac{\partial^2 \theta}{\partial x^2} \tag{11}$$

The target is taken as being semi-infinite; $\theta(\infty,t) = 0$. For first layer heating, the boundary condition at the front surface is

$$\rho c \alpha \frac{\partial \theta(0,t)}{dx} = E_R R$$

Using Laplace transform techniques,[5] the solution of this equation is straightforward. For constant residual energy, the temperature is given by

$$\theta_1(x,t) = Q\left[2\sqrt{\left(\frac{\alpha t}{\pi}\right)}e^{-\eta^2} - x\,\mathrm{erfc}(\eta)\right] \tag{12}$$

where $Q = E_R R/(\rho c\alpha)$ and $\eta = x/(2\sqrt{\alpha t})$. In the case of the variable residual fluence we obtain

$$\theta_1(x,t) = \theta_v(1+\delta)[\mathrm{erfc}(\eta) - \exp(\xi x + \xi^2\alpha t)\,\mathrm{erfc}(n + \xi\sqrt{\alpha t})] \tag{13}$$

where

$$\xi = \left(\frac{E_{R_0}R}{\rho c\alpha}\right)\Big/\theta_v$$

In the case of the front surface reaching vaporization, the boundary condition becomes

$$\theta(0,t') = \theta_v \quad t' = t - t_v$$

The rate of vaporization is assumed small, allowing the fixed boundary approximation to be used. As a consequence of the preheating of the material we can approximate the temperature distribution through the material as

$$\theta(x,t') = \theta_v e^{-x/\lambda_v}$$

This exponential approximation of Eqs. (12) and (13) is excellent at low heating rates. At high heating rates it becomes less accurate, but the total deposited energy becomes small, allowing for reasonable accuracy in the subsequent heating of the material. The solution in this case gives

$$[\theta_2(x,t')]/\theta_v = \{\mathrm{erfc}(\eta) + \tfrac{1}{2}e^{-\eta^2}[f(\omega-\eta) - f(\omega+\eta)]\} \tag{14}$$

where $f(y) = \exp(y)^2\mathrm{erfc}(y)$ and $\omega = \sqrt{\alpha t/\lambda_v}$.

In the limit of $t_v \to 0$, $\lambda \to 0$ this reduces to

$$\theta_2(x,t) = \theta_v \mathrm{erfc}(\eta) \tag{15}$$

For subsequent layer removal, the initial condition of $\theta(h,t_D) = \theta_D$ has to be satisfied. At such time the temperature through the material behind the upper layer can again be well approximated by

$$\theta(x',t_D) = \theta_D e^{-x'/\lambda_D}; \quad x' = x - h$$

At this point in time the thermal contact between the first and second layer is assumed broken, and conduction of the energy into the bulk of the target continues, with no further heat addition, until the first layer is removed from the target. This gives a boundary condition

$$\frac{\partial\theta(0,t_1)}{\partial x} = 0 \quad t_1 = t - t_D$$

The solution to this takes the form

$$\theta_3(x,t') = \tfrac{1}{2}\theta_D e^{-\eta^2}[f(\omega+\eta) + f(\omega-\eta)] \tag{16}$$

On removal of the layer at time $t_1 = \tau$, this approximates to

$$\theta_3(x',\tau) = \theta_R e^{-x'/\lambda_R}$$

which is now the initial condition for subsequent heating of the second layer.

The subsequent heating of the new upper layer is thus characterized by a prior heating component. The constant residual energy model gives solution

$$\theta_4(x,t) = \theta_1(x,t) + \tfrac{1}{2}\theta_R e^{-\eta^2}[f(\omega+\eta) + f(\omega-\eta)] \tag{17}$$

and the variable residual model gives

$$\theta_4(x,t) = \theta_1(x,t) + \theta_R\left(\frac{\xi\lambda_R}{\xi\lambda_R - 1}\right)\exp(\xi x + \xi^2\alpha t)\,\mathrm{erfc}(\eta + \xi\sqrt{\alpha t}) + \tfrac{1}{2}\theta_R e^{-\eta^2}\left\{f(\omega-\eta) + \frac{1+\xi\lambda_R}{1-\xi\lambda_R}f(\omega+\eta)\right\} \tag{18}$$

With the preceding equations it is now possible to solve the complete time history of the heating of a target undergoing delamination. However, at sufficiently high heating rates, the vaporization of the target dominates. Under such circumstances the upper limit of heating rate for delamination to occur is given by

$$t_D = t_v = [(c\theta_v + E_v)/\phi_{\mathrm{abs}}]\rho h$$

where E_v is the heat of vaporization. The minimum delamination time under such circumstances is given by Eq. (15), such that

$$\theta_D/\theta_v = \mathrm{erfc}(h/\{2\sqrt{\alpha t_{HT}}\})$$

Model Predictions

Using the above mathematical formulation it becomes straightforward to compute the layer removal times, and number of pulses, vs the laser repetition frequency. Figure 6 illustrates the influence of layer conduction losses. This example of constant residual fluence, with immediate layer removal on reaching the delamination temperature, clearly shows the difference between first layer and asymptotic limit removal times. The first layer removal time can be seen to have a minimum of 60 Hz where the conduction to energy deposition ratio becomes a minimum. At higher repetition frequencies, the surface reaches vaporization temperature and heat transfer becomes limited. Under these circumstances, conduction into the material becomes insignificant and first layer removal approaches the asymptotic limit.

The variation of asymptotic limit with average flux (repetition frequency × fluence/pulse) can be seen in Fig. 7.

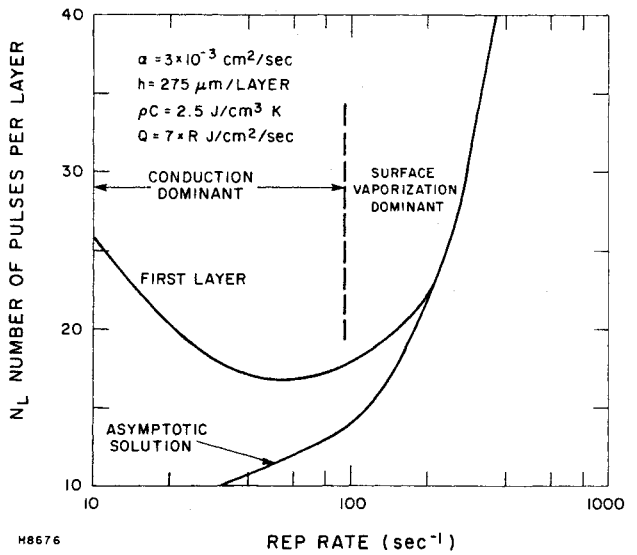

Fig. 6 Predictions of number of pulses to delaminate a layer for constant residual fluence model.

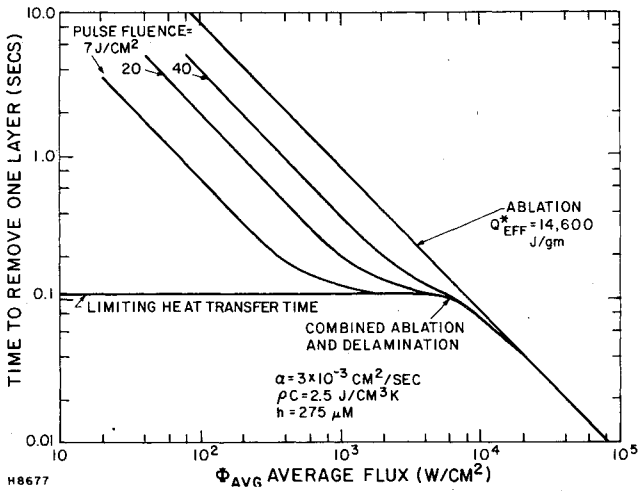

Fig. 7 Phenomenology map of delamination and vaporization for constant residual fluence model.

By increasing the pulse fluence above the residual fluence limit, the excess energy is put into vaporization which is inefficient. Thus, for a given average flux, the greater the pulse fluence above the residual limit, the larger the delamination time. In the limit of low repetition frequency and large fluence, the ablative limit is reached. For a given fluence, an increase in the repetition frequency results in the removal time reaching the limiting heat transfer time [cf Eq. (19)] At higher fluxes vaporization becomes the dominant mechanism for removal of the layer. It is possible, at suitable fluxes, for an ablative thinning of the layer to result in a reduction in the limiting heat transfer time. Thus,

$$t_D \simeq \zeta^2 t_{HT} \simeq (\zeta^2 h^2/4\alpha) g \tag{19}$$

where

$$\theta_D/\theta_v = \operatorname{erfc}(g)$$

and ζ is the effective layer thickness ratio on delamination as a consequence of ablative thinning. Then we can approximate the removal time by

$$(1-\zeta) t_v \simeq \zeta^2 t_{HT} \tag{20}$$

giving solution

$$t_D \simeq t_v \left\{ 1 - \frac{1}{2} \frac{t_v}{t_{TH}} \left[\left(1 + 4 \frac{t_{HT}}{t_v} \right)^{1/2} - 1 \right] \right\} \tag{21}$$

As can be seen in Fig. 7 this effect is not particularly significant.

Comparison with Experimental Data

As has been described earlier, the values of the relevant variables are not accurately known. Typically the thermal diffusivity of fiberglass is in the range $1\text{-}4 \times 10^{-3}$ cm^2/s[6]. The delamination temperature appears to be of order 1000 K. The model was therefore used to evaluate the number of pulses required for the onset first layer delamination over a range of values of α and θ_D.

There is no consistent range of both α and θ_D that fits both 10 and 30 pps data for the constant residual fluence model. However, the variable fluence model provides a remarkably consistent range of values for both delamination time and front surface temperature. Figure 8 illustrates the number of pulses to the onset of delamination as a function of assumed delamination temperature and thermal diffusivity. The hatching in the figure roughly corresponds to the range of acceptable values of these parameters consistent with either 10 or 30 pps data. The region of cross hatching where both 10

EXPERIMENTAL 10 PPS, 33 ± 3 \\\\
30 PPS, 30 ± 3 ////

DELAMINATION TEMPERATURE (K)	THERMAL DIFFUSIVITY 1 x 10^{-3}	2 x 10^{-3}	3 x 10^{-3}	4 x 10^{-3}	REP RATE
900	16.8	18.2	20.8	23.7	10
	20.9	17.9	16.8	17.0	30
1000	21.5	24.0	28.0	32.5	10
	25.4	21.8	21.5	22.0	30
1100	27.0	31.4	37.2	43.6	10
	30.7	27.0	27.0	28.1	30
1200	33.7	40.6	48.9	57.9	10
	37.2	33.1	33.7	35.7	30

Fig. 8 Estimation of parameter values for first layer delamination data; variable residual fluence model.

EXPERIMENTAL 10 PPS ≃ 1330 K ± 80 \\\\
30 PPS ≃ 1480 K ± 80 ////

DELAMINATION TEMPERATURE (K)	THERMAL DIFFUSIVITY (CM^2/SEC) 1 x 10^{-3}	2 x 10^{-3}	3 x 10^{-3}	4 x 10^{-3}	REP RATE
900	1370	1150	1060	1030	10
	1830	1510	1340	1240	30
1000	1460	1250	1180	1130	10
	1895	1580	1420	1330	30
1100	1540	1340	1250	1220	10
	1950	1660	1500	1430	30
1200	1715	1420	1350	1330	10
	2015	1730	1580	1520	30

Fig. 9 Estimation of parameter values from front surface temperature prior to delamination; variable residual fluence model.

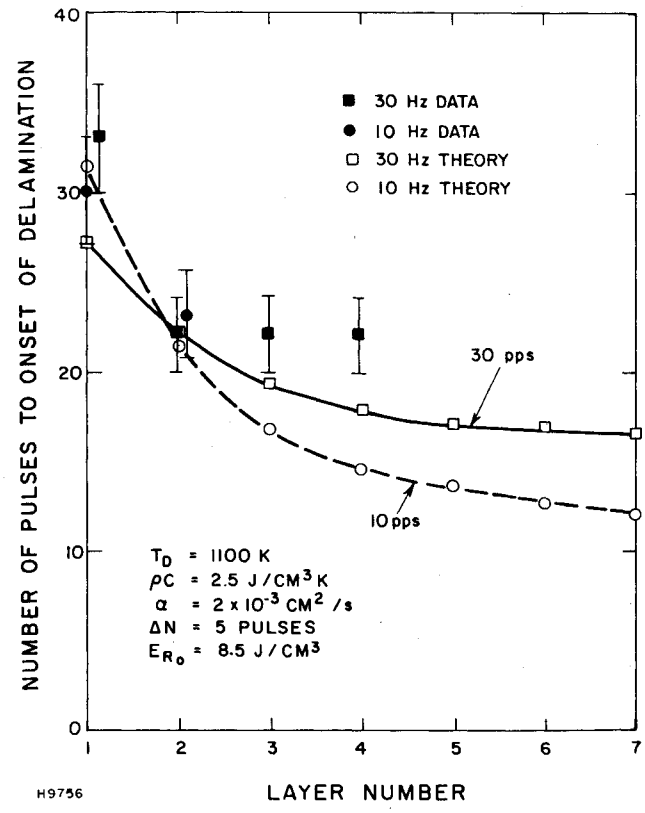

Fig. 10 Comparison of model with 10 and 30 pps delamination data.

and 30 pps data compare favorably with the model is limited to values of $\theta_D \simeq 1100$ K, $\alpha \approx 2\text{-}3 \times 10^{-3}$ cm/s^2. The predicted temperatures at the onset of delamination are shown in Fig. 9. As can be seen, there is again a range of consistent values of α and θ_D that match well with the delamination time data.

A consistent picture emerges from this comparison. It should be noted that slight variations in specific heat and residual fluence values can lead to changes in the predicted values of α and θ_D required for consistency with the data. However, the agreement is sufficiently good for extrapolation to higher average fluxes and repetition frequencies.

Using the inferred values, a comparison was made with the multilayer delamination observations (Fig. 10). Agreement is good for the removal of the first two layers, but becomes divergent for subsequent layers. This is expected as the targets were only six layers thick, and comparison with the semi-infinite modeling is expected to lead to differences. A remaining question is why the finite target takes longer to delaminate than the model would suggest. The answer is likely to be the result of two mechanisms. Firstly, the spatial nonuniformity of the layer breakup and removal process will affect the thermal history of the target, and therefore the subsequent delamination of underlying layers. Secondly, the targets may have a variable delamination criterion as opposed to the constant θ_D approach used in the model. If the criterion is not only one of resin removal, but also of resin removal rate, such as would be required by a pressure induced layer failure, a finite target thickness could lead to the deeper layers having a requirement for a higher layer temperature for removal.

A further illustration of the model's utility is shown in Fig. 11. Here a series of targets with varying laminate thickness was irradiated, which were all epoxy glass composites, but with some minor variations in composition. As can be seen the model compares well with the data.

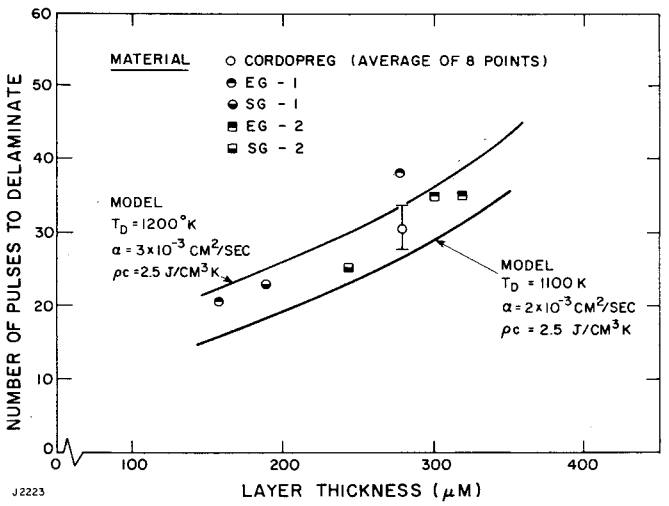

Fig. 11 Comparison of model with first layer delamination data for varying thickness laminate.

Extrapolation to Higher Average Fluxes

Using the values of parameters extracted from the data comparison, extrapolation was made to describe the behavior of target penetration at higher average fluxes. Figure 12 illustrates the behavior of such a laser. The hatched band has an upper bound corresponding to the consistency analysis of the previous section. The lower bound, corresponding to the constant residual fluence model, is included because of the uncertainty of the detailed laser interaction under very high heating rates. However, as described earlier, it is apparent that the upper bound is a more realistic prediction, not withstanding the impact of additional mechanisms, such as melt splash or melt shear flow, under the higher surface temperatures expected at such heating rates.

At high average fluxes, the removal time becomes fixed by heat transfer limitations imposed by the surface reaching vaporization temperature. Increasing the pulse fluence above the residual fluence level results in eventual change from delamination to vaporization mechanisms. With a short pulse length these high fluences will result in plasma formation above the target (see, for example, Refs. 7 and 8) as a consequence of which the coupling of radiation to the surface is reduced. Thus the thermal coupling reduction increases the flux range over which delamination will occur, as opposed to vaporization. At frequencies above 100 Hz the constant residual fluence lower bound approaches the heat transfer limiting value.

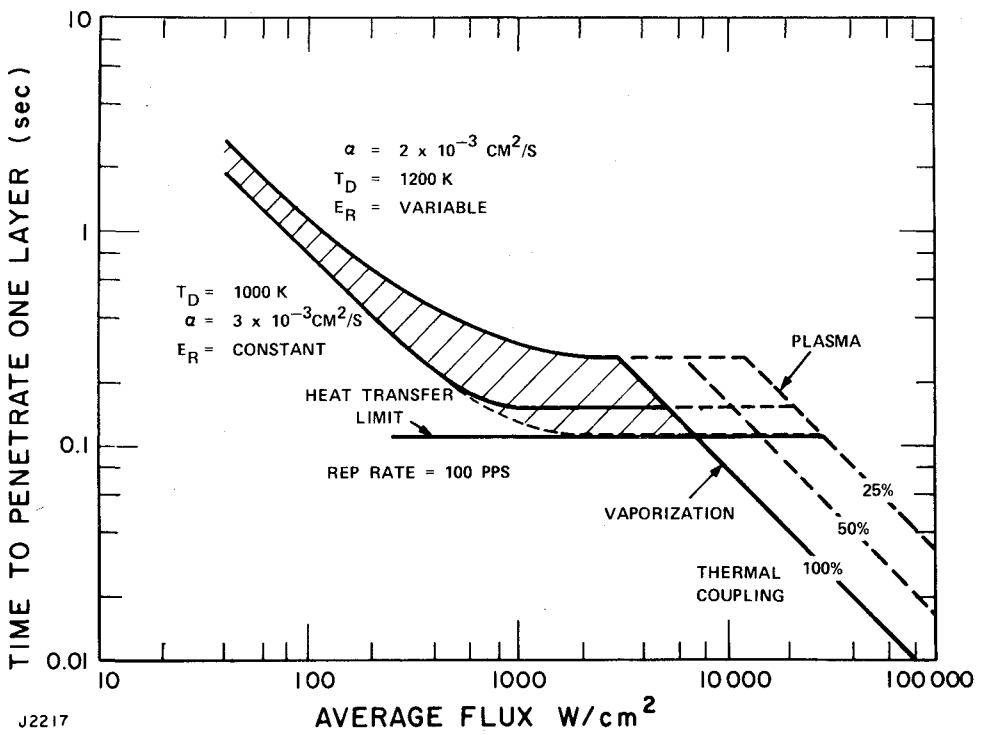

Fig. 12 Extrapolation of model to high average power irradiation.

Summary and Conclusion

An analytical model of the phenomenology of pulsed CO_2 laser interaction with reinforced composite materials has been developed. Good agreement has been obtained between the model predictions and the data base. The observed delamination behavior has been shown to be controlled by the conduction and pyrolysis behavior inside the target. The extrapolation to high average fluxes and repetition frequencies has shown that the control of heat flux into the target by surface vaporization leads to a limiting value of delamination time. At higher fluxes, the delamination process is superseded by vaporization. Changes in target properties, such as laminate thickness, have been shown to correlate well with the model.

Acknowledgment

This work was supported by the United States Army under Contract DAAK40-79-C-0008.

References

[1] Wu, P. K. and Root, R. G., "Single Pulse Laser Irradiation of Fiberglass," *AIAA Journal*, Vol. 18, July 1980, p. 857.

[2] Root, R. G., Pirri, A. N., Wu, P. K., and Gelman, H., "Analysis of Laser Target Interaction," Vol. I, Physical Sciences Inc., TR-170A, March 1979.

[3] Weyl, W. A. and Marboe, E. C., "The Constitution of Glasses," *Intersciences*, Vol. II, Pt. I, 1964.

[4] Edwards, O. J., "Optical Absorption Coefficients of Fused Silica in the Wavelength Range 0.17 to 3.5 Microns from Room Temperature to 980°C," NASA TN D3257, 1966.

[5] Carslaw, H. S. and Jaeger, J. C., *Conduction of Heat in Solids*, Oxford, Clarendon Press, 1959.

[6] Touloukian, Y. S. and Ho, C. Y., "Thermophysical Properties of Selected Aerospace Materials" Pt. II, Thermophysical and Electronic Properties Information Analysis Center/CINDAS, Purdue University, 1977.

[7] Pirri, A. N., Root, R. G., and Wu, P. K., "Plasma Energy Transfer to Irradiated Metal Surfaces by Pulsed Lasers," *AIAA Journal*, Vol. 16, Sept. 1978, p. 1296.

[8] McKay, J. A., Schriempf, J. T., Cronburg, T. L., Eninger, J. E., and Woodroffe, J. A., "Pulsed CO_2 Laser Interaction with a Metal Surface at Oblique Incidence," *Applied Physics Letters*, Vol. 36, Jan. 1980, p. 125.